

## Diffusion and Permeation of Oxygen, Nitrogen, Carbon Dioxide, and Nitrogen Dioxide through Polytetrafluoroethylene

R. A. Pasternak, M. V. Christensen, and J. Heller

*Polymer Chemistry Department, Stanford Research Institute,  
Menlo Park, California 94025. Received December 19, 1969*

**ABSTRACT:** The permeation of  $\text{CO}_2$ ,  $\text{O}_2$ ,  $\text{N}_2$ , and  $\text{N}_2\text{O}_4$ - $\text{NO}_2$  equilibrium mixtures through polytetrafluoroethylene (PTFE) has been investigated systematically. PTFE membranes between 1.5 and 5.7 mil thick were studied over a temperature range of 30–116°. For all the gases, the permeation and diffusion coefficients were found to be independent of membrane thickness, within the precision of the measurements. Linear Arrhenius plots were obtained for  $\text{CO}_2$ ,  $\text{O}_2$ , and  $\text{N}_2$ . For the  $\text{N}_2\text{O}_4$ - $\text{NO}_2$  system, the temperature dependence of both permeation and diffusion was complex; the permeation data could be explained quantitatively in terms of the  $\text{N}_2\text{O}_4$ - $\text{NO}_2$  equilibrium. The parameters describing the diffusion and solution process indicate that the  $\text{CO}_2$ ,  $\text{O}_2$ ,  $\text{N}_2$ , and  $\text{N}_2\text{O}_4$  molecules do not significantly interact with PTFE but move through preexisting channels and voids, whereas  $\text{NO}_2$  interacts strongly, though reversibly, with the polymer.

The development of advanced liquid propulsion systems requires the use of expulsion bladders for storable propellants in the space environment. The bladder material must not only be chemically inert toward strong oxidants such as nitrogen dioxide but must also have a very low permeability toward these agents. Because of its chemical resistance and good mechanical properties, polytetrafluoroethylene (PTFE) has received serious consideration as a bladder material and several space vehicles have been launched using PTFE expulsion bladders.

However, permeation of oxidants through PTFE, while not detrimental in short missions, is of serious concern in long missions. Since only very limited data for the diffusion and permeation of noncondensable gases and none for nitrogen dioxide through PTFE are found in the literature,<sup>1,2</sup> a systematic study of these gases was undertaken in an attempt to understand the details of the interaction between permeants and PTFE.

### Experimental Section

The dynamic method for measuring permeation and diffusion rates of gases and vapors in polymer membranes has been described in detail elsewhere<sup>3</sup> and is here only summarized. The two compartments of the permeation cell, which are separated by the test membrane, are open to the atmosphere. The permeant, gas or vapor, is admitted to one compartment replacing a carrier gas, usually helium. A second carrier gas stream flows at constant rate through the other compartment and sweeps the permeant, which diffuses through the membrane, to the thermal conductivity detector. The detector signal, which is originally zeroed with the carrier gas in both compartments, is at any instant proportional to the permeation rate. When the permeant is again replaced by the carrier gas, the membrane is degassed, and the signal returns to the base line. Thus, repeat measurements can be made with the same membrane over a wide temperature range and for diverse permeants.

The instrument used in this study is a prototype of the polymer permeation analyzer (PPA) (Dohrmann Instrument Co. (Infotronics), Mt. View). The cell and the plumbing were stainless steel; the effective membrane area was 3.9  $\text{cm}^2$ . The detector was a Loenco thermal conductivity cell (Dohrmann Instrument Co.) which was run at 140 mA and thermostated at 80°. Its sensitivity for  $\text{CO}_2$ , 144 ppm/mV, did not change significantly with time, even after exposure to  $\text{NO}_2$ . The combination of the detector with a Sargent recorder (full scale deflection of 250 mm at an input of 0.4 mV) resulted in a detection limit of 0.2 ppm of  $\text{CO}_2$  in helium. Helium was used as carrier gas for the study of all permeants, except of hydrogen, for which nitrogen was used. (With  $\text{N}_2$  as carrier gas the detector current was 50 mA.) The flow rates of the carrier gas were set between 0.5 and 1.5 ml/sec, the higher values being employed at high diffusion rates. At steady-state permeation, strict inverse proportionality between signal and flow rate was found as expected for a detector with linear response.

The detector sensitivity, which is a function of the gas or vapor sensed, was determined for  $\text{CO}_2$  and  $\text{H}_2\text{O}$ . Helium with 0.21 vol %  $\text{CO}_2$  and nitrogen with 0.20 vol %  $\text{H}_2$  were used as test gases. Moreover, the permeation rates of  $\text{CO}_2$ ,  $\text{O}_2$ , and  $\text{N}_2$  through a PTFE membrane were measured in a Barrer-type permeation cell (Linde Model CS 135), and compared with the equivalent signals obtained in the PPA. The permeation coefficients for  $\text{CO}_2$  derived by the two independent approaches differed by 7%; the data reported here are based on the calibration of the PPA. The mole response factors of the detector for  $\text{O}_2$  and  $\text{N}_2$  (relative to  $\text{CO}_2$ ) were found to be 1.20 and 1.22; the factor for  $\text{NO}_2$  was assumed to be unity because its molecular weight differs by only two units from that of  $\text{CO}_2$ . No  $\text{N}_2\text{O}_4$  reached the detector since in the helium stream the highest partial pressure of the nitrogen oxides, expressed as  $\text{NO}_2$ , was less than 0.1%. Finally, the equilibrium solubility of  $\text{N}_2\text{O}_4$ - $\text{NO}_2$  in PTFE at a total pressure of 1 atm was measured over a limited temperature range with a quartz spring balance.

High purity  $\text{CO}_2$ ,  $\text{O}_2$ , and  $\text{N}_2$  were used without further purification or drying; the  $\text{N}_2\text{O}_4$ - $\text{NO}_2$  mixture was bled into the cell from a tank held at 30°. The PTFE used in this study had a density of 2.18 g/cc at 18° as determined by immersion in water. Membranes were cut with a microtome from a solid polymer block of Du Pont Teflon, commercial stock, and their thicknesses were determined by a micrometer with a reading precision of 0.05 mil. Only membranes with thickness variation of less than 5% were used.

**Evaluation of Permeation and Diffusion Coefficients.** In Figure 1a a typical permeation curve for  $\text{CO}_2$  is shown. The

(1) W. W. Brandt and G. A. Ansysas, *J. Appl. Polym. Sci.*, **7**, 1919 (1963).

(2) Modern Plastics Encyclopedia, Vol. 45, No. 1A, McGraw-Hill Book Co., Inc., New York, N. Y., 1968, p 532.

(3) R. A. Pasternak, J. F. Schimscheimer, and J. Heller, *J. Polym. Sci., Part A-2*, in press.

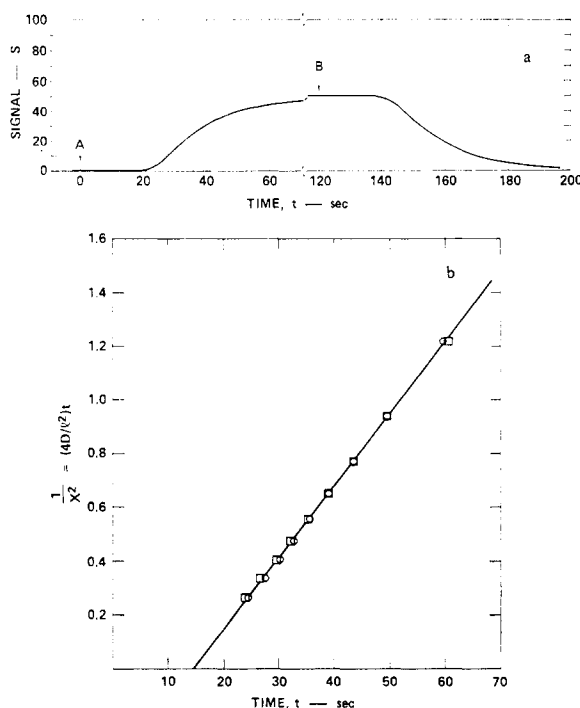


Figure 1. (a) Experimental curve for permeation of  $\text{CO}_2$  through a 4.3-mil PTFE membrane at  $90.6^\circ$ , arbitrary units.  $\text{CO}_2$  was introduced at A; He at B. (b) Plot of  $1/X^2$  vs. time  $t$  at  $S/S_\infty = 0.1, 0.2, \dots, 0.9$ :  $\circ$ , ascending branch;  $\square$ , descending branch.

plateau represents steady-state permeation. The permeation coefficient  $P$  is calculated by the formula

$$P = \frac{f\sigma k a S_\infty l}{A p} \left( \frac{\text{cc cm}}{\text{cm}^2 \text{ sec cm}} \right)$$

where  $f$  is the flow rate,  $\sigma$  the detector sensitivity,  $k$  the molecular response factor,  $a$  the detector attenuation,  $S_\infty$  the steady-state signal,  $l$  the membrane thickness,  $A$  the membrane area, and  $p$  the upstream permeant pressure. The permeant pressure is taken as 76 cm although it varied slightly.

The steady-state data for  $\text{N}_2\text{O}_4\text{-NO}_2$  are reported as the measured flow of  $\text{NO}_2$  at a total pressure of 1 atm, normalized to unit area and thickness. Formalistically, the flux is identical with a nominal permeation coefficient at atmospheric pressure.

The diffusion coefficient was derived from the ascending and descending branches of Figure 1a which represent the transient permeation rates. The solution of the differential equation describing the transient state has been discussed in detail elsewhere.<sup>8</sup> It is to a good approximation

$$\frac{S}{S_\infty} = \frac{4}{\sqrt{\pi}} X \exp(-X^2)$$

where  $X^2 = l^2/4Dt$ ,  $S$  is the signal at time  $t$ , and  $D$  is the concentration-independent diffusion coefficient. This equation describes both sorption and degassing, which are identical except for reversal in the direction of the signal. A plot of  $S/S_\infty$  vs.  $1/X^2$  is the theoretical, normalized, permeation rate curve. If, for the same values of  $S/S_\infty$ , the normalized times  $1/X^2$  are plotted vs. the experimental times  $t$ , the straight line through the origin should have a slope equal to  $4D/l^2$ . Figure 1b represents this evaluation of the ascending and descending branches of Figure 1a. The points lie on a straight line, and close agreement is found between the two

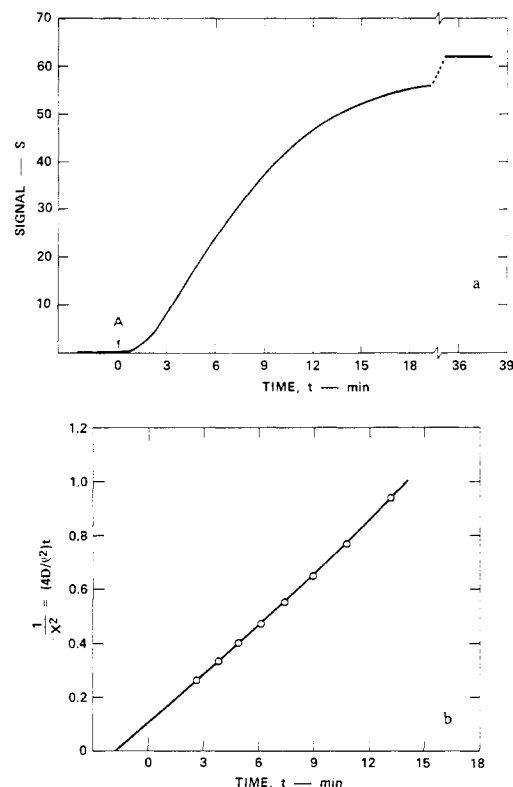


Figure 2. (a) Experimental curve for permeation of  $\text{N}_2\text{O}_4\text{-NO}_2$  through a 4.3-mil PTFE membrane at  $49.7^\circ$ , arbitrary units. (b) Plot of  $1/X^2$  vs. experimental time  $t$  at  $S/S_\infty = 0.1, 0.2, \dots, 0.8$ .

branches. However, a positive displacement on the time axis is found, because a finite time is required for the permeant to reach the upper compartment, and for the permeated gas to reach the detector.

A simplified method has been adopted for the evaluation of the large amount of data. The slope, which is given by the ratio  $\Delta(1/X^2)/\Delta t$ , was evaluated from two sets of two experimental points each, namely for  $S/S_\infty = 0.1, 0.4$ , and  $S/S_\infty = 0.4, 0.7$ . For the noncondensable gases, the two values agreed within 5% and were averaged.

For the  $\text{NO}_2\text{-N}_2\text{O}_4$  system the determination of diffusion coefficients by the described formalism becomes questionable. The simultaneous diffusion of two interacting components must result in a complex rate law; unfortunately, the differential equation cannot be solved explicitly in this case. The experimental curves have shapes similar to those for the noncondensable gases (Figure 2a); however, plots of  $1/X^2$  vs.  $t$  (Figure 2b), though approximately linear, show a slight curvature and they intercept the time axes at negative values. Both effects diminish with increasing temperature, as would be expected from a consideration of the  $\text{N}_2\text{O}_4\text{-NO}_2$  equilibrium. The nominal diffusion coefficients reported here were somewhat arbitrarily derived from the slopes for the interval  $S/S_\infty = 0.1, 0.4$ .

## Results and Discussion

**1. Carbon Dioxide, Oxygen, and Nitrogen.** In Figure 3 the logarithm of the permeation coefficients for  $\text{CO}_2$ ,  $\text{O}_2$ , and  $\text{N}_2$  derived from the data are plotted vs.  $1/T$ ; Figure 4 is an equivalent plot of the diffusion coefficients. For  $\text{CO}_2$ , membranes of thickness 1.5, 3.2, 3.5, 4.3, and 5.7 mil were used, but no diffusion coefficients are given for the thinnest membrane, since the transient permeation rates were too fast to yield

TABLE I<sup>a</sup>  
 DIFFUSION, PERMEATION, AND SOLUBILITY DATA FOR NONCONDENSABLE GASES IN PTFE

	$D_{25} \times 10^7$	$D_0 \times 10^3$	$E_D$	$P_{25} \times 10^9$	$P_0 \times 10^6$	$E_P$	$s_{25} \times 10^2$	$s_0 \times 10^4$	$\Delta H_s$	$P_{25} \times 10^9$
CO <sub>2</sub>	0.95	1.03	6.84	1.17	0.33	3.34	1.230	0.323	-3.50	1.00
O <sub>2</sub>	1.52	0.64	6.28	0.42	0.93	4.55	0.276	1.48	-1.73	0.45
N <sub>2</sub>	0.88	1.52	7.12	0.14	2.69	5.82	0.159	1.76	-1.30	0.19
H <sub>2</sub>				0.98		5.10				1.30

<sup>a</sup>  $D_{25}$  and  $D_0$  in cm<sup>2</sup>/sec;  $P_{25}$  and  $P_0$  in cc(STP) cm/cm<sup>2</sup> sec cm;  $s_{25}$  and  $s_0$  in cc(STP)/cm<sup>3</sup> cm;  $E$  and  $\Delta H$  in kcal/mol. The diffusion coefficient at absolute temperature  $T$  is given by  $D = D_0 \exp(-E_D/RT)$ . Analogous expressions apply to the permeation coefficient  $P$  and the solubility  $s$ . The subscript 25 signifies the value at 25°. <sup>b</sup> FEP, ref 2.

reliable values. The 1.5-mil membrane was omitted in the O<sub>2</sub> and N<sub>2</sub> studies.

The complete data cover a temperature range of 30–116°; however, the individual membranes were studied over smaller intervals, the range depending on the membrane thickness. Also, for any given membrane, permeation coefficients are usually given to higher temperatures than diffusion coefficients because the determination of the latter becomes unreliable for fast transient rates.

Since the agreement between the data for different membranes was very good, they were all combined in a least square treatment. The straight lines in the figures represent the results. The mean square root deviation of the individual data points from the best line is between 3 and 5% for all plots. Deviations for an individual membrane do not appear to be systematic or significant, and are well within the range of uncertainties originating from thickness measurement and slight variation in flow rate of the carrier gas.

In Table I the diffusion and permeation coefficients at 25°,  $D_{25}$  and  $P_{25}$ , the preexponential factors  $D_0$  and  $P_0$ , and the heats  $E_D$  and  $E_P$ , are summarized. In addition, the solubility coefficients calculated from  $s = P/D$  are listed. The permeation coefficient and the heat of permeation of H<sub>2</sub>, which was measured for one membrane only and at four temperatures between 24 and 48°, are included. Permeation coefficients for

the four gases in the similar FEP given in the literature<sup>2</sup> are shown also.

The diffusion and permeation coefficients of CO<sub>2</sub>, O<sub>2</sub>, and N<sub>2</sub>, plotted in Figures 3 and 4, confirm convincingly that the generally assumed simple diffusion law holds; the independence of the coefficients on membrane thickness, in particular, proves that the sorption process on the membrane surface is fast and is not the rate-determining step. The data also show that the activation energies of diffusion and permeation are independent of temperature, over the rather wide temperature range of this study.

The activation energies of diffusion  $E_D$  of the three gases (Table I) are quite similar. However, in view of the high precision of the data, the differences, though small, are significant. This is also indicated by the trend in the preexponential factors; their logarithms, *i.e.*, the entropies of activation, are approximately a linear function of the activation energies of diffusion, as has been found in other systems.<sup>1</sup> The trend in  $E_D$  appears to be associated with the molecular sizes of the gases. Oxygen has a significantly smaller van der Waal's diameter (2.92 Å) than N<sub>2</sub> (3.15 Å) and CO<sub>2</sub> (3.32 Å).<sup>4</sup> Moreover, since the cross-section perpendicular to the molecular axis is smaller for CO<sub>2</sub> than for

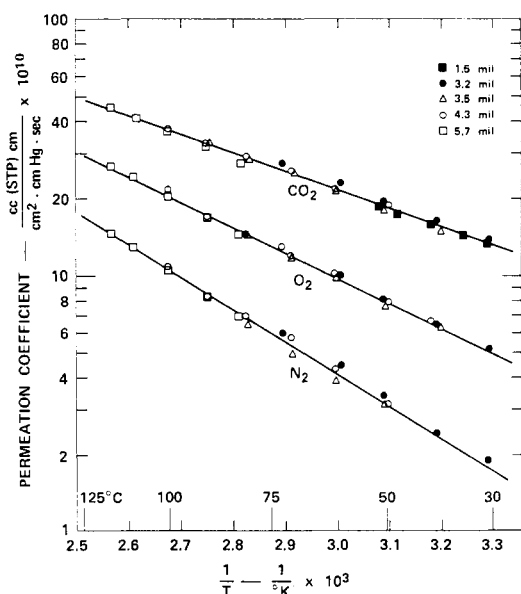


Figure 3. Arrhenius plots of permeation coefficients in PTFE.

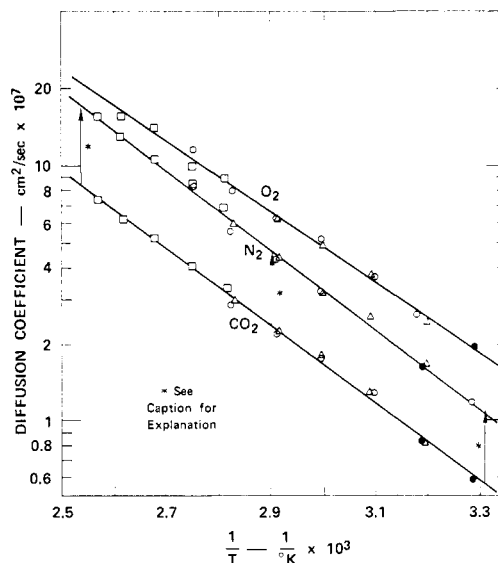


Figure 4. Arrhenius plots of diffusion coefficients in PTFE. The CO<sub>2</sub> curve is shifted by a factor of 2: □, 5.7 mil; ○, 4.3 mil; ●, 3.2 mil.

(4) "Handbook of Chemistry and Physics," 36th ed, Chemical Rubber Publishing Co., Cleveland, Ohio, 1955, p 3094.

TABLE II<sup>a</sup>  
DIFFUSION AND SOLUBILITY DATA OF PTFE (T) AND  
OF LINEAR POLYETHYLENE (PE)<sup>b</sup>

	$E_D$		$s_{25} \times 10^2$		$\Delta H_s$		
	T	PE	T	PE	T	PE	$\Delta H_{\text{cond}}$
CO <sub>2</sub>	6.84	8.5	3.1	0.60	-3.50	-1.3	-4.0 <sup>c</sup>
O <sub>2</sub>	6.28	8.8	0.69	0.10	-1.73	-0.4	-1.6
N <sub>2</sub>	7.12	9.0	0.39	0.054	-1.30	0.5	-1.3

<sup>a</sup>  $\Delta H$  in kcal/mol;  $s_{25}$  in cc(STP)/cm<sup>3</sup> cm. <sup>b</sup> Reference 5. <sup>c</sup> At triple point, -56°.

TABLE III  
SOLUBILITY IN PTFE OF N<sub>2</sub>O<sub>4</sub>-NO<sub>2</sub> EQUILIBRIUM  
MIXTURE AT 1 ATM PRESSURE

T, °C	$s$ , g/cc atm		$s$ , cc NO <sub>2</sub> - (STP)/cc atm (average)
	Sample 1	Sample 2	
30.1	0.039	0.038	19.0
35.4	0.027		13.0
40.6	0.019	0.020	9.5

N<sub>2</sub>, the lower  $E_D$  value for CO<sub>2</sub> may indicate that the molecules permeate by preference in the direction of their molecular axis.

The heats of solution of the three gases in PTFE and their heats of condensation (last column) are compared in Table II. The close numerical agreement is probably fortuitous; nevertheless it indicates that solution in PTFE is similar to a condensation process with minimal interaction between the polymer and the solute.

A comparison of diffusion and solubility data of PTFE with those of the structurally similar linear polyethylene is of some interest (Table II). The polyethylene data are for a Phillips type 22% amorphous polymer and are taken from two papers by Michaels and Bixler;<sup>5</sup> they are converted to the units used here. The solubilities refer to the amorphous phase and are calculated assuming the solubility in the crystalline phase to be negligible. The PTFE used was 40% amorphous as determined from its density.

The activation energy of diffusion of the three gases in PTFE is about 2 kcal/mol lower than in polyethylene. This is surprising, since PTFE has very stiff backbone chains of high viscosity. Apparently, as proposed originally by Brandt and Anysas,<sup>1</sup> diffusion of small molecules in this polymer proceeds through preformed channels and cavities and requires little movement of the polymer chains.

The higher gas solubilities at 25°, more than six times those in polyethylene, and the higher heats of solution may again indicate poor packing of the PTFE chains in the amorphous regions. A part of the difference, however, may be due to the difference in cohesive energy density of the two polymers. The solubilities of N<sub>2</sub>, O<sub>2</sub> and CO<sub>2</sub> in perfluoroheptane, for example, are larger by a factor of 2-3 than in heptane.<sup>6</sup> Further study is required to establish the relative significance of the two effects.

(5) A. S. Michaels and H. T. Bixler, *J. Polym. Sci.*, **50**, 393, 413 (1961).

(6) J. H. Hildebrand and R. L. Scott, "Regular Solutions," Prentice-Hall, Englewood Cliffs, N. J., 1962, pp 47 and 162.

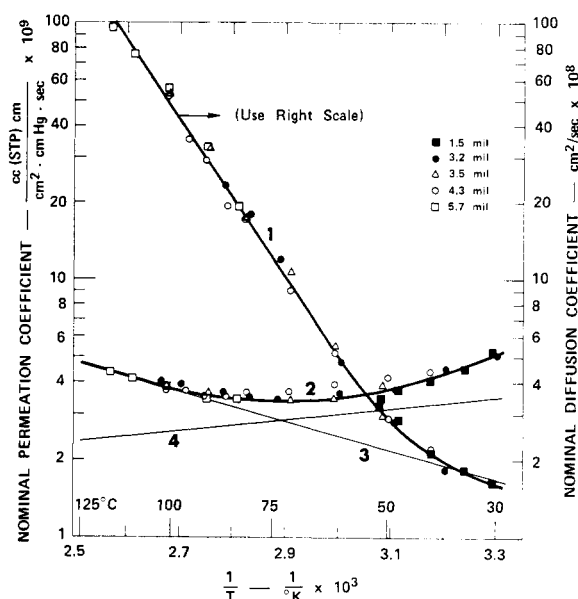


Figure 5. Permeation and diffusion coefficients of N<sub>2</sub>O<sub>4</sub>-NO<sub>2</sub> equilibrium mixtures in PTFE: (1) nominal diffusion coefficients of mixture; (2) nominal permeation coefficients of mixture; (3) permeation coefficients of NO<sub>2</sub>; (4) permeation coefficients of N<sub>2</sub>O<sub>4</sub>.

**2. Nitrogen Dioxide.** Figure 5 summarizes the data for the N<sub>2</sub>O<sub>4</sub>-NO<sub>2</sub> system obtained with the same five membranes as for CO<sub>2</sub>. Repeat runs were reproducible even after long time exposure of the membranes to the strong oxidant. Moreover, data for CO<sub>2</sub> obtained before and after exposure to NO<sub>2</sub> were identical within the precision of the measurements, evidence that PTFE is not attacked by NO<sub>2</sub>. The nominal diffusion coefficients (see preceding section) lie on a straight line (curve 1) except at the lower temperatures. The steady-state permeation data closely fit the theoretical curve 2 (see below), except for some points for the 4.3-mil membrane at lower temperatures.

Finally, in Table III the solubilities of the N<sub>2</sub>O<sub>4</sub>-NO<sub>2</sub> equilibrium mixtures at a total pressure of 1 atm are given for two PTFE samples; the agreement is quite satisfactory.

The close agreement of the apparent diffusion coefficients and the normalized permeation rates for different membrane thicknesses, shown in Figure 5, indicate again that the adsorption process is fast, and that the transport within the membrane is the rate-determining step. This transport mechanism however is complex not only because two species diffuse, but also because the relative concentrations of N<sub>2</sub>O<sub>4</sub> and NO<sub>2</sub> in the gas phase and in the polymer are functions of temperature and total pressure (or concentration).

The equilibrium in the gas phase is given by<sup>7</sup>

$$\frac{(p_{\text{NO}_2})^2}{p_{\text{N}_2\text{O}_4}} = K_p = 7.1 \times 10^9 \exp \frac{-14,600}{RT} \text{ atm} \quad (1)$$

At a total pressure of 1 atm on the upstream side of the membrane (our standard experimental condition)

(7) F. H. Getman and F. Daniels, "Physical Chemistry," John Wiley & Sons, Inc., New York, N. Y., 1946, p 297.

TABLE IV  
DIFFUSION, PERMEATION, AND SOLUBILITY DATA FOR NO<sub>2</sub> AND N<sub>2</sub>O<sub>4</sub> IN PTFE  
(FOR UNITS AND DEFINITIONS, SEE TABLE II)

	$D_{25} \times 10^7$	$D_0$	$E_D$	$P_{25} \times 10^9$	$P_0 \times 10^6$	$E_P$	$s_{25} \times 10^2$	$s_0 \times 10^9$	$\Delta H_s$
NO <sub>2</sub>	0.037	70	14.0	1.57	0.116	2.55	43	1.66	-11.4
N <sub>2</sub> O <sub>4</sub>	0.25			3.75	0.0013	-0.5	15		

the partial pressure of NO<sub>2</sub> is 0.36 atm at 30°, and 0.99 atm at 116°. (On the downstream side, virtually pure NO<sub>2</sub> is released since the total pressure of permeant in the helium stream was in all experiments below 10<sup>-3</sup> atm.)

Since at the highest temperatures of this study the gas phase consists of virtually pure NO<sub>2</sub>, it is reasonable to assume that the measured nominal diffusion and permeation coefficients are the true coefficients for NO<sub>2</sub>. Actually, the diffusion coefficient curve is at the higher temperatures linear over a much wider interval than anticipated. The diffusion parameters derived from it are ascribed to NO<sub>2</sub> and listed in Table IV.

In our analysis of the observed nonlinear temperature dependence of permeation, we make the following postulates: (1) the solubility of either component obeys Henry's law

$$C_i^0 = s_i p_i \quad (2)$$

where  $C_i^0$  is the saturation concentration in the polymer,  $s_i$  is the solubility coefficient, and  $p_i$  is the pressure in the gas phase; (2) both the diffusion and solubility coefficients are independent of concentration. This postulate probably holds only approximately since the total equilibrium amount of NO<sub>2</sub> + N<sub>2</sub>O<sub>4</sub> dissolved at the lowest temperature of the experimental series is about 2% by weight; (3) the equilibrium N<sub>2</sub>O<sub>4</sub> ⇌ 2NO<sub>2</sub> is maintained at all times in the gas phase and everywhere within the membrane, even during transient permeation.

It follows from the three postulates that the concentrations  $C_i$  anywhere in the polymer satisfy, at all times, the equilibrium condition

$$\frac{(C_{\text{NO}_2})^2}{C_{\text{N}_2\text{O}_4}} = K_e = K_p \frac{s_{\text{N}_2\text{O}_4}}{(s_{\text{NO}_2})^2} \quad (3)$$

Diffusion through the membrane is described by the two differential equations

$$\frac{dC_{\text{NO}_2}}{dt} = -D_{\text{NO}_2} \frac{d^2 C_{\text{NO}_2}}{dx^2} + 2R \quad (4a)$$

$$\frac{dC_{\text{N}_2\text{O}_4}}{dt} = -D_{\text{N}_2\text{O}_4} \frac{d^2 C_{\text{N}_2\text{O}_4}}{dx^2} - R \quad (4b)$$

$R$  is the net rate of conversion of N<sub>2</sub>O<sub>4</sub> to NO<sub>2</sub>; the factor 2 in eq 4a accounts for the production of two NO<sub>2</sub> molecules for every dissociating N<sub>2</sub>O<sub>4</sub> molecule.

Equations 4a and 4b are not independent, but are related by eq 3. By combining these three equations, a differential equation in  $C_{\text{NO}_2}$ , time  $t$ , and position  $x$  can be obtained. Unfortunately, this equation cannot be solved except numerically, and therefore the diffusion coefficients cannot be derived explicitly from the experimental curves. However, a solution can be obtained for the steady state, when the concentrations

of both NO<sub>2</sub> and N<sub>2</sub>O<sub>4</sub> anywhere in the membrane are independent of time. The flux  $F$  of permeant through the membrane of thickness  $l$

$$F = -D_{\text{NO}_2} \frac{dC_{\text{NO}_2}}{dx} - 2D_{\text{N}_2\text{O}_4} \frac{dC_{\text{N}_2\text{O}_4}}{dx} \quad (5)$$

is then constant, *i.e.*, also independent of  $x$ . The factor 2 has been introduced to express the flux in terms of the NO<sub>2</sub> species, which appears exclusively on the downstream side of the membrane.

At steady state the boundary conditions are

$$\text{at } x = 0 \quad C_{\text{NO}_2} = C_{\text{NO}_2}^0$$

$$C_{\text{N}_2\text{O}_4} = C_{\text{N}_2\text{O}_4}^0$$

$$\text{at } x = l \quad C_{\text{NO}_2} = C_{\text{N}_2\text{O}_4} = 0$$

Integration of eq 5 between these limits yields

$$Fl = D_{\text{NO}_2} C_{\text{NO}_2}^0 + 2D_{\text{N}_2\text{O}_4} C_{\text{N}_2\text{O}_4}^0 \quad (6)$$

On introducing Henry's law, eq 1, we obtain

$$Fl = D_{\text{NO}_2} s_{\text{NO}_2} p_{\text{NO}_2} + 2D_{\text{N}_2\text{O}_4} s_{\text{N}_2\text{O}_4} p_{\text{N}_2\text{O}_4} \quad (7)$$

We define the flux at unit thickness  $F_0 = Fl$ , and the permeation coefficients  $P_{\text{NO}_2} = D_{\text{NO}_2} s_{\text{NO}_2}$ ,  $P_{\text{N}_2\text{O}_4} = D_{\text{N}_2\text{O}_4} s_{\text{N}_2\text{O}_4}$ . Since in our experiments the pressure condition holds,  $p_{\text{NO}_2} + p_{\text{N}_2\text{O}_4} = 1$  atm, the flux equation assumes the simple form

$$F_0 = p_{\text{NO}_2} P_{\text{NO}_2} + 2(1 - p_{\text{NO}_2}) P_{\text{N}_2\text{O}_4} \quad (8)$$

Formalistically this equation is identical with the expression that describes the permeation of two independent components; however, in the NO<sub>2</sub>-N<sub>2</sub>O<sub>4</sub> case, the concentrations of the two species in the membrane are not linear functions of  $x$  but are related by the mass law.

It can be easily seen that the permeation data plotted in Figure 5 are in the form of this normalized flux  $F_0$ ; they can be analyzed in terms of eq 8. We postulate that both  $P_{\text{NO}_2}$  and  $P_{\text{N}_2\text{O}_4}$  show an exponential dependence on the reciprocal temperature. Since at the highest temperatures of the experiments the gas phase is virtually pure NO<sub>2</sub>, the permeation coefficients  $P_{\text{NO}_2}$  are given by the asymptote to the high-temperature data, curve 3 in Figure 5, and can be extrapolated to lower temperatures. Moreover, the partial pressures of  $p_{\text{NO}_2}$  are given by equilibrium eq 1. Consequently, only the permeation coefficient  $P_{\text{N}_2\text{O}_4}$  of eq 8 is unknown and can be calculated at different temperatures from the smoothed, experimental  $F_0$  values. After minor adjustments in the slope of the  $P_{\text{NO}_2}$  curve, a linear  $P_{\text{N}_2\text{O}_4}$  curve was obtained [(4) in Figure 5]. Then, as a check, the total flux  $F_0$  was recalculated from the two permeation curves (3) and (4). The agreement of the calculated curve (2) with the experimental data is excellent, except for some points derived from the 4.3-mil membrane.

The parameters derived from the two permeation curves (3) and (4) are listed in Table IV. The coefficients, which in Figure 5 are given in atmospheric pressure units, are converted to centimeters to facilitate comparison with the CO<sub>2</sub>, O<sub>2</sub>, and N<sub>2</sub> data. Approximate solubility and diffusion coefficients of N<sub>2</sub>O<sub>4</sub> at 25° are given also. The solubility coefficient was derived from the directly measured solubilities (Table II) by extrapolation to 25°. A correction was made for the solubility of the NO<sub>2</sub> present in the gas phase at 25°.

A comparison of the solubility and diffusion coefficients of N<sub>2</sub>O<sub>4</sub> and of CO<sub>2</sub>, O<sub>2</sub>, N<sub>2</sub> indicates a common pattern. The solubility coefficients of the gases correlate quite well with their boiling points, as has been found for other gas-polymer systems.<sup>8</sup> Similarly, the reduction in the N<sub>2</sub>O<sub>4</sub> diffusion coefficient by a factor of about 4 compared to CO<sub>2</sub> appears to be reasonable in view of the much larger size of the N<sub>2</sub>O<sub>4</sub> molecule. Thus, N<sub>2</sub>O<sub>4</sub>, like the other gases, apparently does not interact with PTFE.

In contrast, the NO<sub>2</sub> data do not fit the pattern

(8) G. T. van Amerongen, *Rubber Chem. Technol.*, **37**, 1065, (1964).

at all. Although the NO<sub>2</sub> molecule has approximately the same size as CO<sub>2</sub>, its activation energy of diffusion is about twice and its heat of solution about three times that of CO<sub>2</sub>. Also, its diffusion and solubility coefficients at 25° are smaller and larger, respectively, by orders of magnitude. These observations suggest that the highly polar NO<sub>2</sub> molecule interacts strongly with PTFE.

A systematic analysis of the data in terms of molecular dimensions and interchain forces is not only of considerable interest, but is essential for a more detailed and quantitative understanding of diffusion mechanisms. This analysis must however be postponed until data for a larger number of permeants and PTFE samples of different degree of crystallinity are available.

**Acknowledgment.** The authors are indebted to Mr. David D. Lawson for suggesting this research and for preparing suitable membranes. This work was performed for the Jet Propulsion Laboratory, California Institute of Technology, sponsored by the National Aeronautics and Space Administration under Contract NAS 7-698.

## Notes

### Validity of the Gaussian Approximation to the Polymer Scattering Factor in Simple Chain Models<sup>1</sup>

ARTURO HORTA

*Institute of Physical Chemistry "Rocasolano" (CSIC), Madrid 6, Spain. Received December 9, 1969*

The particle scattering factor  $P$ , for an isolated polymer chain in equilibrium, can be written as

$$P(\omega) = \frac{1}{N^2} \sum_{i=1}^N \sum_{j=1}^N \left\langle \frac{\sin \omega r_{ij}}{\omega r_{ij}} \right\rangle \quad (1)$$

$N$  being the total number of scattering elements in the chain,  $r_{ij}$  the distance between elements  $i$  and  $j$ , and  $\omega = (2\pi/\lambda)2 \sin(\theta/2)$ , where  $\lambda$  is wavelength and  $\theta$  scattering angle.

When the segment distribution is gaussian, the average in eq 1 can be expressed in terms of the second moment  $\langle r_{ij}^2 \rangle$  of the distribution,<sup>2</sup> and  $P$  reads

$$P(\omega) = \frac{1}{N^2} \sum_{i=1}^N \sum_{j=1}^N \exp\left(-\frac{\omega^2}{6} \langle r_{ij}^2 \rangle\right) \quad (2)$$

However, gaussian statistics represent only a particular behavior of the chain, and many cases of interest correspond to coils with nongaussian effects.

Since very little is known about the form of the distribution for nongaussian coils, a general procedure to calculate  $P$  for such coils is to assume that eq 2

(1) A preliminary report of this work was presented at the XIV Meeting of the Spanish Society of Physics and Chemistry, Sevilla, Oct 1969.

(2) A gaussian distribution does not necessarily imply the random-flight proportionality between  $\langle r_{ij}^2 \rangle$  and  $|i - j|$ . An example of gaussian distribution with more complicated second moment is given by A. Horta, *Eur. Polym. J.*, in press.

is still valid, and to incorporate the nongaussian behavior by substituting for  $\langle r_{ij}^2 \rangle$  a form which adequately represents the actual mean quadratic separation between segments. This *ad hoc* procedure has been extensively used to study the influence on  $P$  of excluded volume,<sup>3-5</sup> chain stiffness,<sup>5,6</sup> and the detailed structure of the chain<sup>7</sup> (represented by the rotational isomeric model). It is, thus, of great interest to estimate the error that is committed by these type of calculations which apply the gaussian form (2) to nongaussian model chains. A step in this direction is the work of Nagai, who showed<sup>8</sup> that, for a generic distribution,  $\langle \sin \omega r_{ij} / \omega r_{ij} \rangle$  can be expanded in a power series whose zeroth order term is the gaussian exponential  $\exp(-\omega^2 \cdot \langle r_{ij}^2 \rangle / 6)$ .

The purpose of this note is to determine, numerically, the error committed with the gaussian approximation (2) in the case of two very simple nongaussian models, for which a closed expression of the exact  $P$  is known. The models are the conditional probability chain (CP) presented by Verstratte and Frankenberg,<sup>9</sup> and the zigzag chain (ZZ) or broken rod.<sup>10</sup>

For a polymer chain consisting of  $N$  elements sepa-

(3) A. J. Hyde, J. H. Ryan, and F. T. Wall, *J. Polym. Sci.*, **33**, 129 (1958).

(4) O. B. Ptitsyn and Y. Y. Eisner, *Vysokomol. Soedin.*, **1**, 966 (1959).

(5) A. Peterlin in "Electromagnetic Scattering," M. Kerker, Ed., Pergamon Press, New York, N. Y., 1963, p 357.

(6) A. Peterlin, *Makromol. Chem.*, **9**, 244 (1953).

(7) P. J. Flory and R. L. Jernigan, *J. Amer. Chem. Soc.*, **90**, 3128 (1968).

(8) K. Nagai, *J. Chem. Phys.*, **38**, 924 (1963).

(9) G. Verstratte and C. v. Frankenberg, *J. Polym. Sci., Part A-2*, **5**, 1313 (1967).

(10) J. E. Hearst and W. H. Stockmayer, *J. Chem. Phys.*, **37**, 1425 (1962).